Supplementary Material

Disruption of spatiotemporal hypoxic signaling causes congenital heart disease

Xuejun Yuan, Hui Qi, Xiang Li, Fan Wu, Jian Fang, Eva Bober, Gergana Dobreva, Yonggang Zhou, Thomas Braun

Max-Planck-Institute for Heart and Lung Research, Department of Cardiac Development and Remodeling, Bad Nauheim Germany

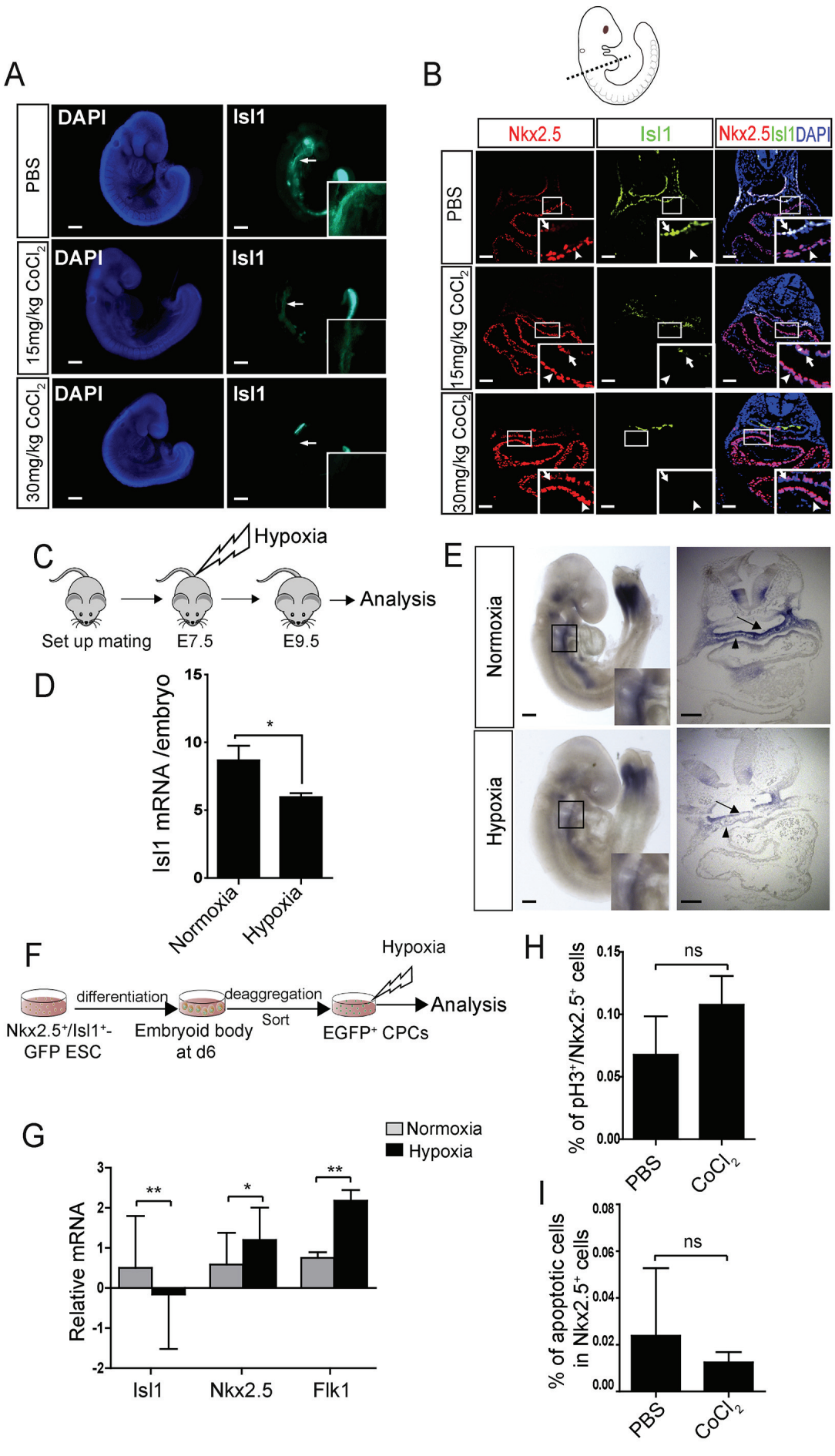
A
PBS
15mg/kg CoCl2
30mg/kg CoCl2
DAPI
Isl1
B
Nkx2.5
Isl1
Nkx2.5Isl1DAPI
C
Hypoxia
Set up mating
E7.5
E9.5
Analysis
D
Isl1 mRNA /embryo
Normoxia
Hypoxia
E
F
differentiation
deaggregation
Sort
Nkx2.5+/Isl1+-GFP ESC
Embryoid body at d6
EGFP+ CPCs
G
Normoxia
Hypoxia
Relative mRNA
Isl1
Nkx2.5
Flk1
H
% of pH3+/Nkx2.5+ cells
ns
PBS
CoCl2
I
% of apoptotic cells in Nkx2.5+ cells
ns
PBS
CoCl2

Supplementary Figure 1: Induction of hypoxia responses represses *Isl1* expression *in vivo*. **(A)** Whole-mount immunostaining of C57/Bl6 E9.0 embryos (14 somites) for Isl1 after chemical induction of hypoxia responses (15 or 30mg $CoCl_2$/kg body weight). Arrows indicate the $Isl1^+$ cardiogenic region. Representative images from 2 independent experiments are shown. Scale bar: 100 μm. **(B)** Representative images of E9.0 (14 somites) C57/Bl6 embryos immunostained for ISL1 and NKX2.5 after $CoCl_2$ treatment are shown. PBS-injected mice were used as control. Arrows indicate cardiac mesoderm and arrowheads indicate the heart tube. Analyzed embryos were randomly selected from two different litters for each condition. Scale bar: 100 μm. **(C)** Scheme of the strategy to induce hypoxia responses during early embryogenesis. Wild-type C57/Bl6 pregnant mice (E7.5) were housed in a hypoxia chamber containing 10% O_2 and 90% N_2 for 48 hrs to induce hypoxia responses *in vivo*. **(D)** RT-qPCR analysis of *Isl1* expression in C57/Bl6 E8.0 embryos (5 somites) after hypoxia exposure. The *m34b4* gene was used as a reference for normalization (t-test: *$p<0.05$, n=3). **(E)** Analysis of *Isl1* expression in C57/Bl6 E9.0 embryos by WISH after hypoxia exposure. Arrows indicate foregut endoderm and arrowheads indicate cardiac mesoderm. Representative images from 2 independent experiments are shown. Scale bar: 100 μm. **(F)** Scheme of the strategy to induce hypoxia responses in $Nkx2.5^+/Isl1^+$-GFP cells isolated from embryoid bodies at day 6. **(G)** RT-qPCR analysis of *Isl1*, *Nkx2.5* and *Flk1* expression in embryoid bodies (EBs) at day 6 after hypoxia exposure for 16 hrs (1% O_2). Please note the down-regulation of *Isl1* (n=7) but up-regulation of *Nkx2.5* (n=3) and *Flk1* (n=4). The *m34b4* gene was used as a reference for normalization. (t-test: *$p<0.05$; **$p<0.01$; $n\geq3$). **(H)** Analysis of $Nkx2.5^+$ cells proliferation in mock or $CoCl_2$ treated E9.5 Nkx2.5-emGFP embryos by immunostaining for phospho-Histone H3 (Ser10) (pH3). The percentages of pH3/GFP double positive cells are shown. At least 3 sections were counted for each embryo (t-test: ns $P>0.05$; n=3). **(I)** TUNEL assay of $Nkx2.5^+$ cells after $CoCl_2$ treatment. The percentage of TUNEL-positive $Nkx2.5^+$ cells is shown. At least 4 sections were counted for each embryo (t-test: ns $P>0.05$; n=3).

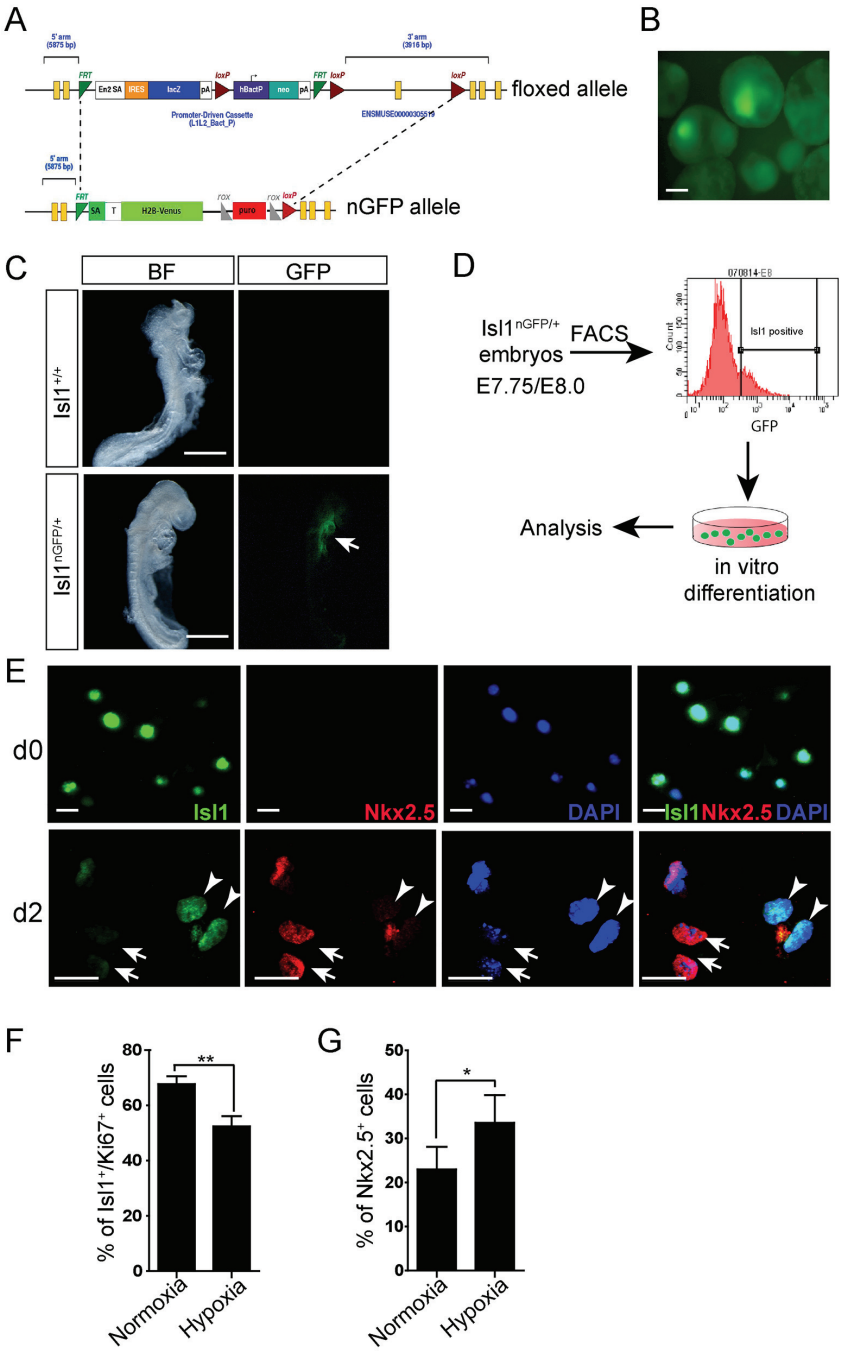

Supplementary Figure 2: Isolation and *in vitro* differentiation of Isl1^{+} CPCs. (A) Scheme of the generation of Isl1$^{nGFP/+}$ reporter mice by dual recombinase-mediated cassette exchange. **(B)** Fluorescence image of GFP positive EBs at day 7 after *in vitro* differentiation of Isl1$^{nGFP/+}$ ES cells. Scale bar: 100 µm. **(C)** Bright field and fluorescence images of control and Isl1$^{nGFP/+}$ embryos at E8.5 (10 somites). Isl1-GFP-positive cells are indicated by an arrow. Scale bar: 200 µm. **(D)** Scheme of Isl1^{+} CPC *in vitro* differentiation after FACS-based isolation. **(E)** Immunofluorescence staining of CPCs for ISL1 and NKX2.5 after 2 days culture in differentiation media. Cultivation in differentiation medium increases the number of Nkx2.5^{+} CPCs. Arrows indicate Isl1^{-}/Nkx2.5^{+} CPCs and arrowheads indicate Isl1^{+}/Nkx2.5^{-} CPCs. Representative images from 3 independent experiments are shown. Scale bar: 100 µm. **(F)** Quantification of proliferating Ki67^{+} (immunostained) CPCs isolated from Isl1^{nGFP} embryos (E8.0 embryos, 5-8 somites) after exposure to normoxia (n=3) or hypoxia (n=4) *in vitro*. (t-test: **p<0.01). **(G)** Quantification of the percentage of Nkx2.5^{+} (immunostained) cells within the population of Isl1^{+} cells after exposure to hypoxia *in vitro*. (t-test: *p<0.05, n=4).

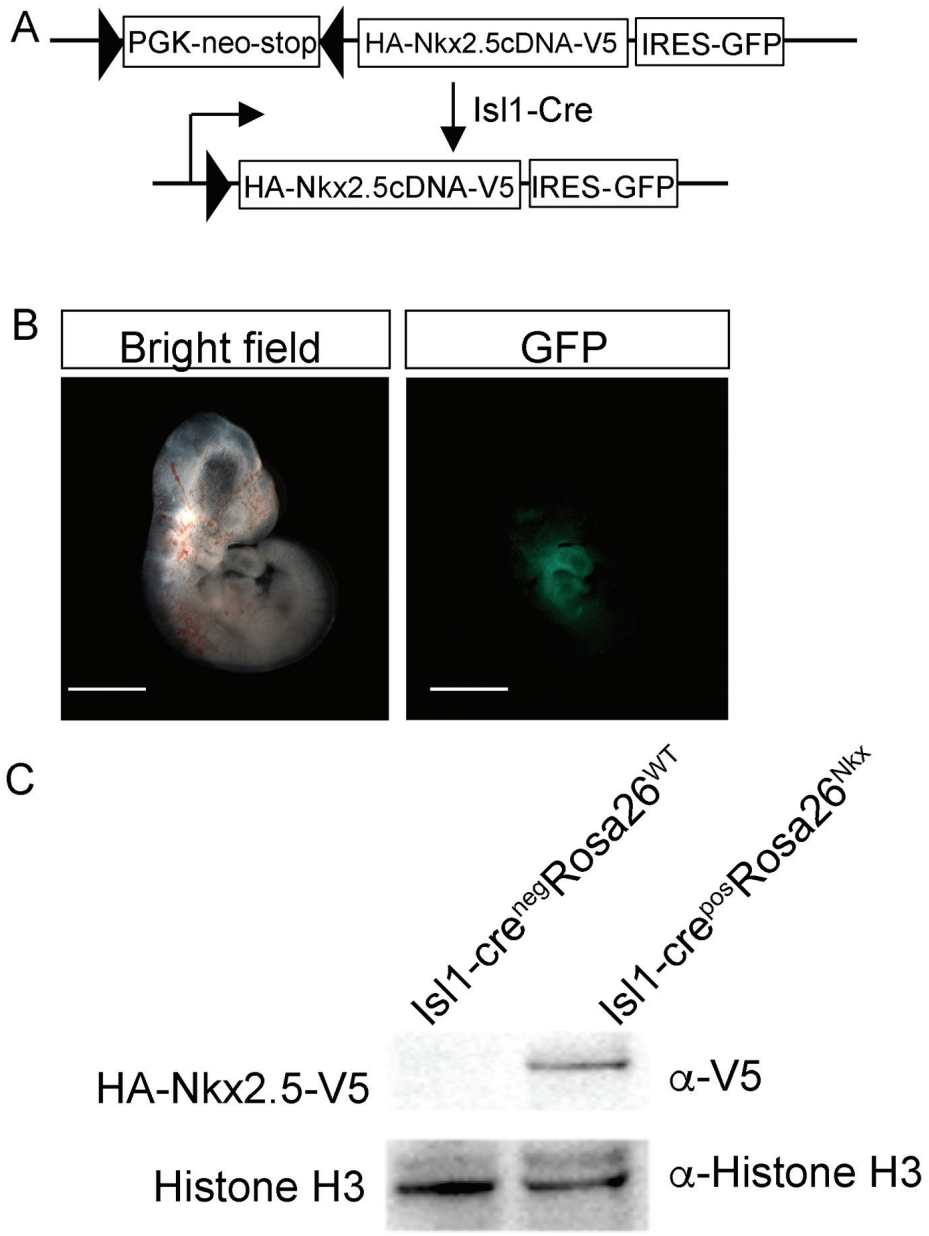

Supplementary Figure 3: Generation of transgenic mice expressing Nkx2.5 in Isl1^{+} cells. **(A)** Outline of the strategy to express *Nkx2.5* in Isl1^{+} cells. **(B)** Bright field and fluorescence images of Nkx2.5-IRES-GFP expression in E10.5 embryos (Isl1-cre^{pos}Rosa26^{Nkx}). Scale bar: 500 µm. **(C)** Western blot analysis to monitor expression of NKX2.5 in Isl1-cre^{pos}Rosa26^{Nkx} embryos at E9.5. Wildtype littermates were used as controls. Histone H3 was used as protein loading control.

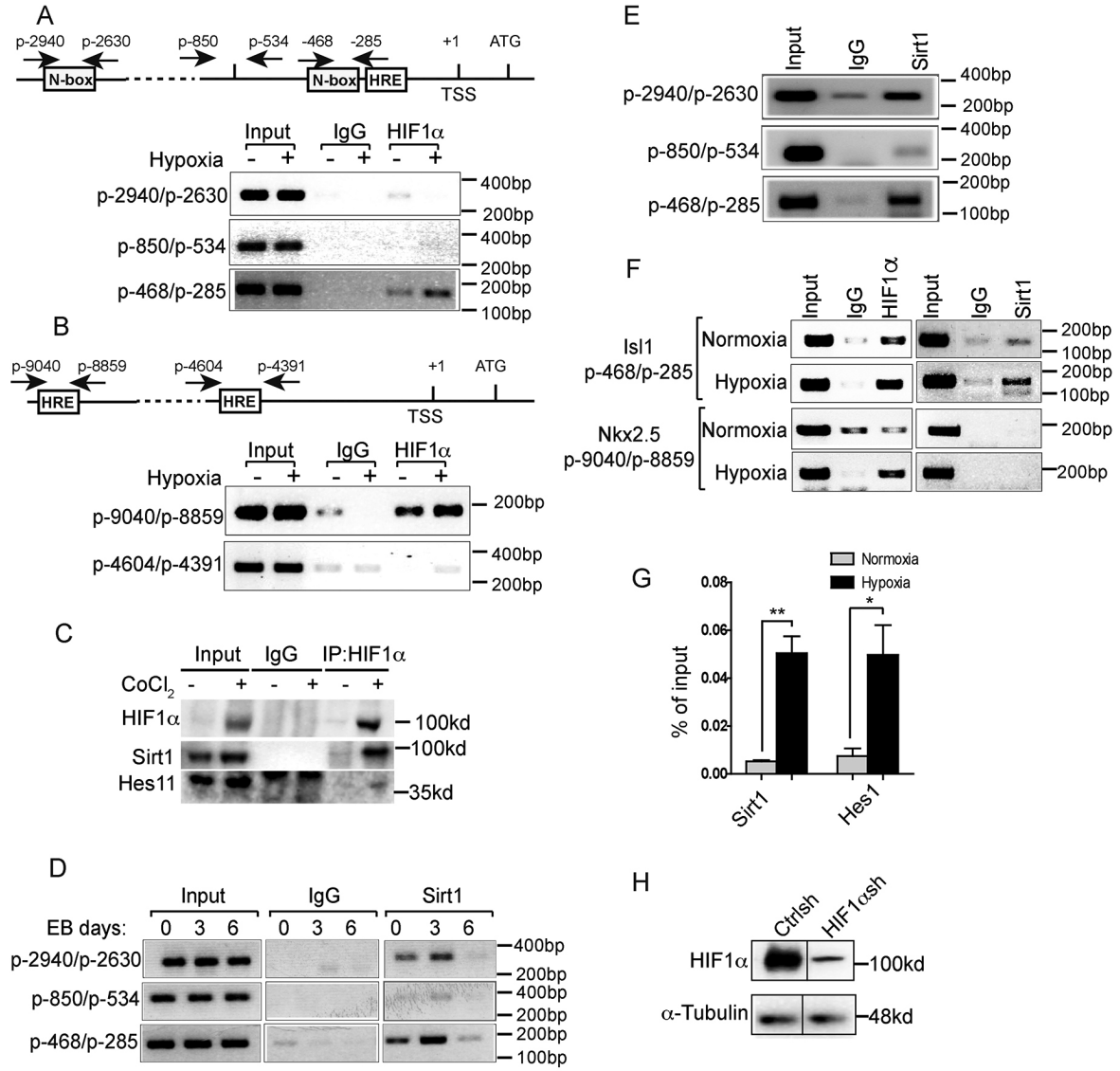

Supplementary Figure 4: Hypoxia enhances binding of Sirt1 to the *Isl1* promoter. (A) ChIP analysis of HIF1α binding to the *Isl1* proximal promoter in differentiating ES cells (EB at day 6) with and without exposure to hypoxia. **(B)** ChIP analysis of HIF1α binding to the *Nkx2.5* distal promoter in differentiating ES cells (EB at day 6). **(C)** Co-IP assay of HIF1α with SIRT1 or HES1 after $CoCl_2$ treatment of V6.5 ES cells. 2.5% input was used. **(D)** ChIP analysis of SIRT1 binding to the *Isl1* proximal promoter in differentiating ES cells at different time points. **(E)** ChIP analyses of SIRT1 binding to the *Isl1* enhancer and proximal promoter in embryonic hearts at E11.5. **(F)** ChIP analysis of HIF1α and SIRT1 binding to *Isl1* and *Nkx2.5* promoters in differentiating ES cells (EB at day 6). Hypoxia enhances binding of HIF1α to the *Isl1* and *Nkx2.5* promoters and increases binding of SIRT1 to the *Isl1* but not the *Nkx2.5* promoter. **(G)** ChIP analysis of SIRT1 and HES1 binding to the *Isl1* proximal promoter in differentiating ES cells without and with exposure to 1% O_2 for 16 hrs. Note increased binding of SIRT1 and HES1 after exposure to hypoxia. The relative enrichment of SIRT1 is normalized against the input DNA. (t-test: *p<0.05; **p<0.01; n=3). **(H)** Western blot analysis of HIF1α levels in differentiating ES cells exposed to $CoCl_2$ after infection with a lentivirus expressing an shRNA against *Hif1α*. α–Tubulin was used as protein loading control. Lanes were run on the same gel but not next to each other.

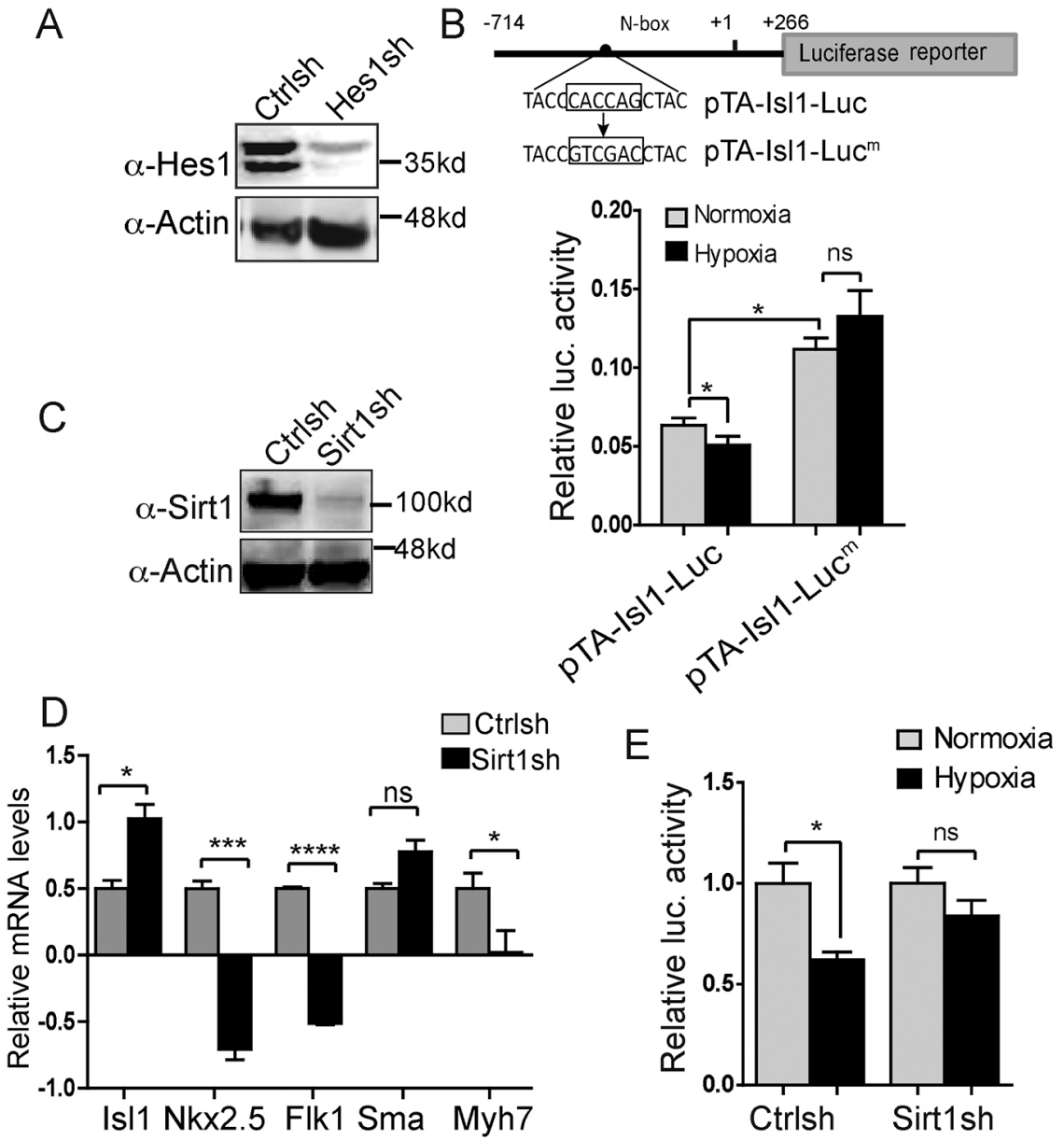

Supplementary Figure 5: A SIRT1-HES1-containing complex mediates down-regulation of *Isl1* expression in CPCs. (A) Western blot analysis of HES1 levels in C2C12 cells after infection with a lentivirus expressing a shRNA against *Hes1*. Actin was used as protein loading control. **(B)** Luciferase reporter assays of *Isl1* WT and N-box mutated promoters in C2C12 cells under normoxia or hypoxia. Mutation of the N-box increases *Isl1* promoter activity and prevents hypoxia-mediated suppression (ANOVA with Tukey's post hoc test: *p<0.05; ns p>0.05; n=3). **(C)** Western blot analysis of SIRT1 protein in V6.5 ES cells after infection with a lentivirus expressing *Sirt1* shRNA. Actin was used as loading control. **(D)** RT-qPCR analysis of *Isl1*, *Nkx2.5*, *Flk1* (EB at E6) and *Sma*, *Myh7* (EB at E8) expression in differentiating V6.5 ES cells after *Sirt1* knockdown. The *m34b4* gene was used as a reference for normalization (t-test: *p<0.05; **p<0.001; ***p<0.0001; ns p>0.05, n=3). **(E)** Luciferase reporter assay of the *Isl1* promoter in C2C12 cells after knockdown of *Sirt1*, with and without exposure to hypoxia. Hypoxia fails to reduce *Isl1* promoter activity in C2C12 cells after *Sirt1* knockdown (t-test: *p<0.05; n=3).

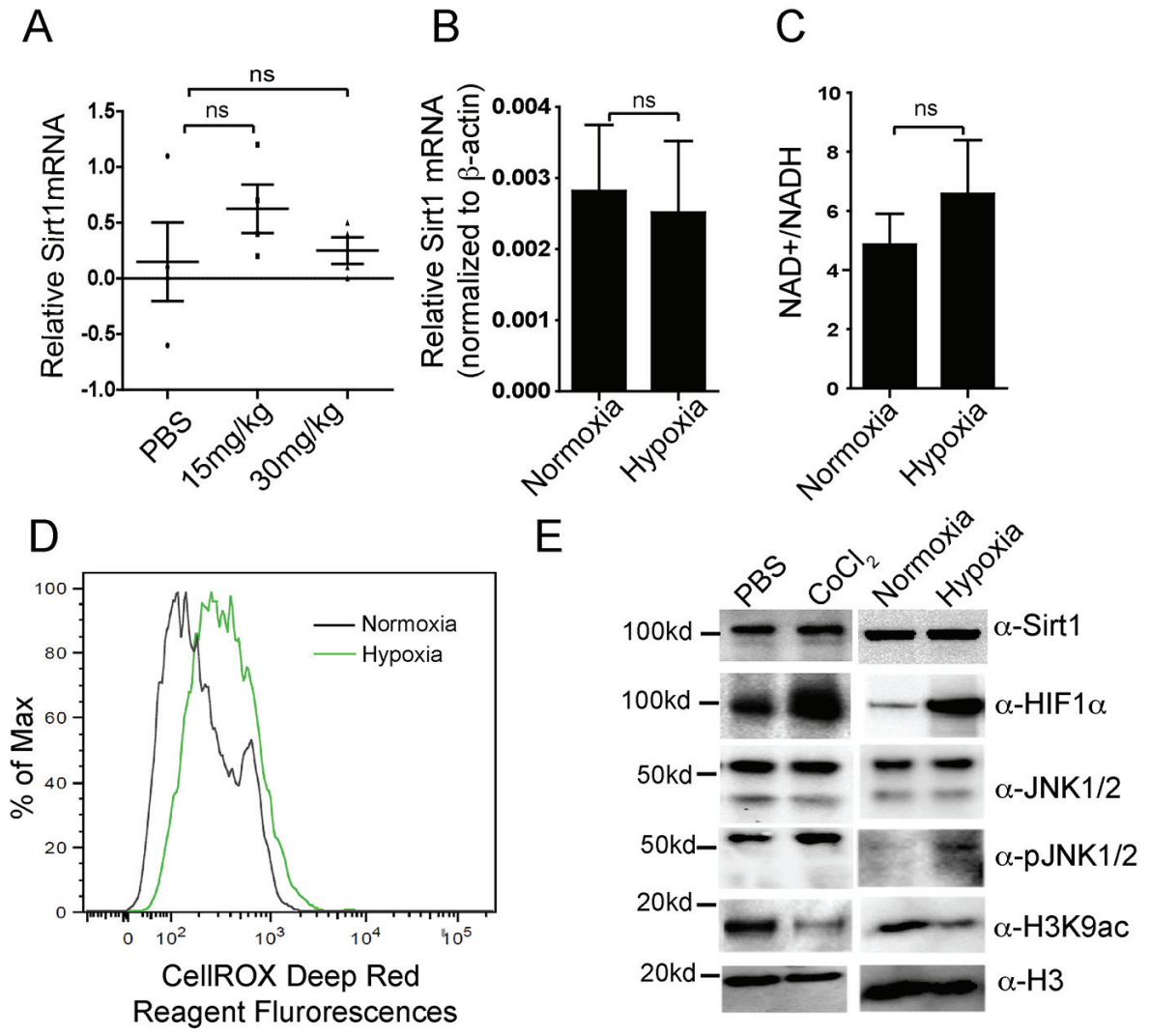

Supplementary Figure 6: Hypoxia responses enhance the activity of SIRT1. (A) RT-qPCR analysis of *Sirt1* expression after chemical induction of hypoxia responses ($CoCl_2$ treatment) in E8.5 embryonic hearts. The *m34b4* gene was used as a reference for normalization. ANOVA with Dunnett's post hoc test was used to calculate significance (ns $p>0.05$; n=4). **(B)** RT-qPCR analysis of *Sirt1* expression in sorted $Isl1^+$ cells after cultivation under normoxia (21% O_2) and hypoxia (1% O_2) for 16 hours. The *β-actin* gene was used as a reference for normalization (t-test: ns $p>0.05$; n=6). **(C)** NAD+/NADH ratios in sorted $Isl1^+$ cells after cultivation under normoxia (21% O_2) and hypoxia (1% O_2) for 16 hours. (t-test: ns $p>0.05$; n=3). **(D)** Cellular ROS levels of sorted $Isl1^+$ cells under hypoxia (1% O_2) and normoxia (21% O_2). Two independent experiments were performed generating similar results. **(E)** Western blot analysis of embryonic hearts isolated from mock (PBS) or $CoCl_2$ treated (15 mg/kg bodyweight) pregnant mice (E8.5, 8-12 somites) and of sorted $Isl1^+$ CPCs exposed to either normoxia (21% O_2) or hypoxia (1% O_2).

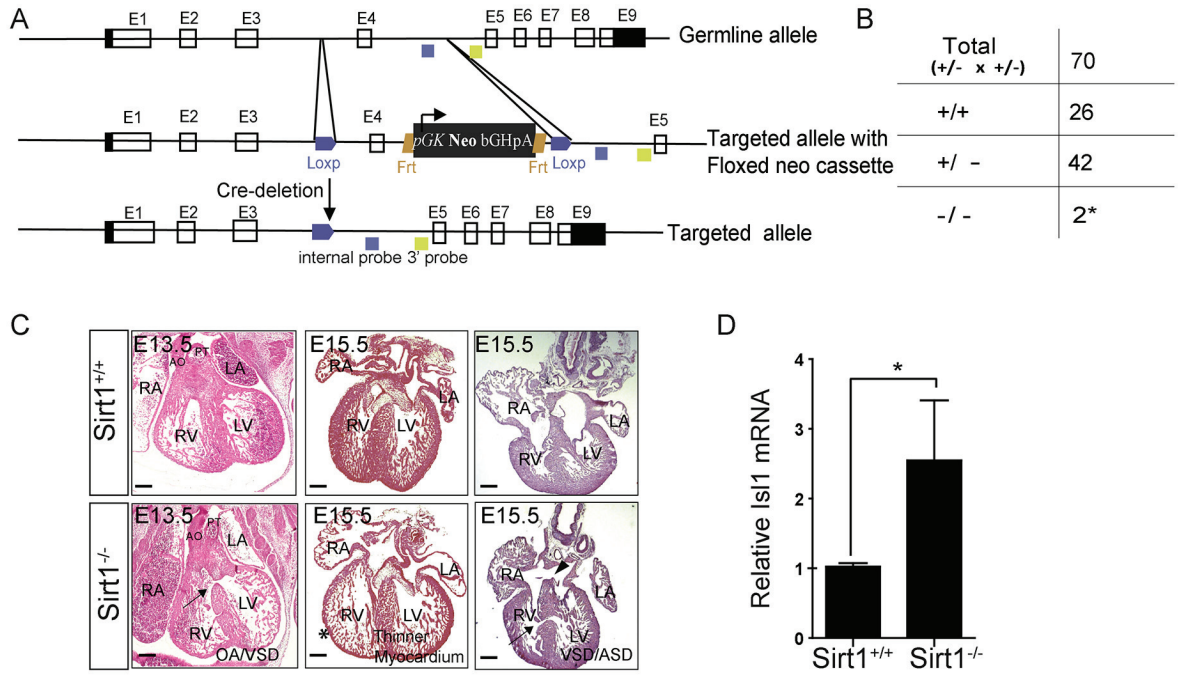

Supplementary Figure 7: Germ line inactivation of *Sirt1* leads to multiple cardiac defects. (A) Outline of the strategy to inactivate the *Sirt1* gene. **(B)** Distribution of genotypes at weaning after breeding of heterozygous *Sirt1* mutant mice. Asterisk indicates that these mice died 2 weeks after birth. **(C)** H&E staining of embryonic hearts from Sirt1$^{+/+}$ (n=6) and Sirt1$^{-/-}$ (n=6) germ line mutants. 6 littermates from 3 different litters were analyzed. Arrows indicate ventricular septum defects (2 out of 6 embryos); arrowhead indicates atrial septum defect (2 out of 6 embryos); Asterisk indicates thinner right ventricular compact layer (4 out of 6 embryos). LA: left atrium; RA: right atrium; LV: left ventricle; RV: right ventricle. Scale bars: 100 μm. **(D)** RT-qPCR analysis of *Isl1* expression in E8.0 (5 somites) Sirt1$^{+/+}$ WT and Sirt1$^{-/-}$ germ line mutants. The *m34b4* gene was used as a reference for normalization (t-test: *p<0.05; n=4 from 2 different litters).

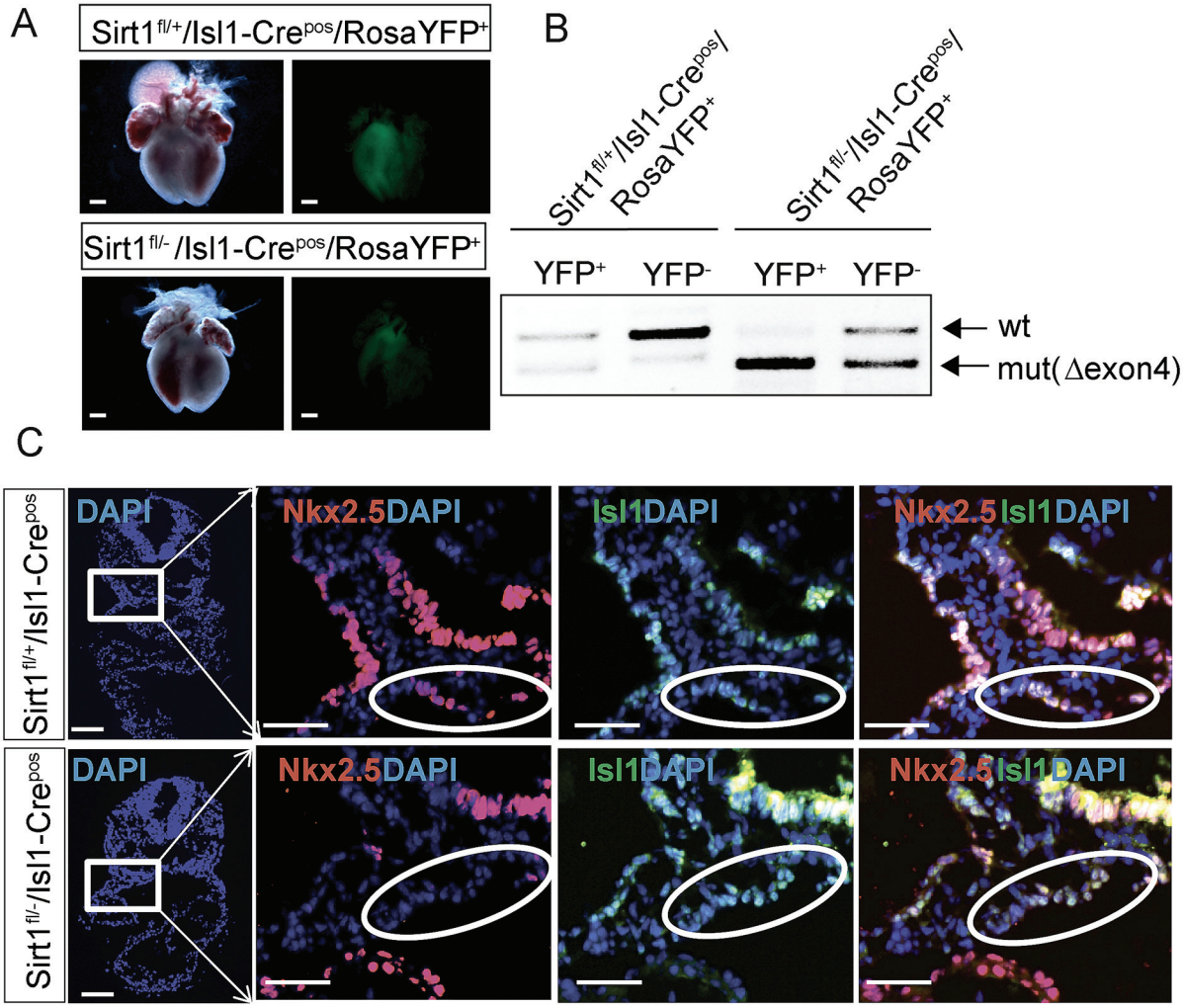

Supplementary Figure 8: Isl1-Cre mediated inactivation of *Sirt1* reduces the number of Isl1^{+}/Nkx2.5^{+} cells in the cardiac mesoderm. (A) Cell tracing of Isl1^{+} CPCs progeny (green) in E15.5 Isl1-Cre^{pos}/Sirt1$^{fl/+}$/RosaYFP^{+} and Isl1-Cre^{pos}/Sirt1$^{fl/-}$/RosaYFP^{+} hearts. Scale bars: 100 µm. **(B)** RT-PCR analysis of WT and mutant *Sirt1* mRNA in Isl1-Cre^{pos}/Sirt1$^{fl/+}$/RosaYFP^{+} and Isl1-Cre^{pos}/Sirt1$^{fl/-}$/RosaYFP^{+} E15.5 hearts after sorting of Isl1^{+} (YFP^{+}) and Isl1^{-} (YFP^{-}) cells. **(C)** Representative immunofluorescence images of cryosections of E9.5 Isl1-Cre^{pos}/Sirt1$^{fl/+}$ and Isl1-Cre^{pos}/Sirt1$^{fl/-}$ hearts stained for ISL1 and NKX2.5 are shown. 3 pairs of *Sirt1* heterozygous and mutant littermates from 2 litters were analyzed. Note the decreased number of Isl1^{+}/Nkx2.5^{+} cells in the cardiac mesoderm after Isl1-Cre mediated knockout of *Sirt1*.

Table S1

Phenotype / Treatment	No obvious defect (%)	Thinner myocardium (%)	Muscular VSD (%)	OA/VSD (%)	DORV (%)	PTA (%)	Abnormal RV dilation or hypoplasia (%)
Low $CoCl_2$ (N=22)	5 (23%)	6 (27%)	7 (32%)	1 (4,5%)	0	0	9 (41%)
High $CoCl_2$ (N=22)	1 (4.5%)	7 (32%)	0	16 (72%)	3 (14%)	1 (4.5%)	6 (27%)

Suppl. Table 1: Incidence of cardiac structural defects in $CoCl_2$ treated C57/Bl6 embryos. Summary of cardiac structural defects in $CoCl_2$ treated embryos detected by H&E staining of paraffin sections from E15.5 mouse hearts. The penetrance of cardiac defects in the $CoCl_2$ treated hearts with variable incidence of different CHDs is indicated. DORV, double outlet right ventricle; VSD: ventricular septal defect; PTA: persistent truncus arteriosus (PTA); OA: overriding aorta.

Table S2

Genotypes \ Phenotypes		No obvious defect	Thinner myocardium	Muscular VSD	OA/VSD	Abnormal RV dilation or hypoplasia
-$CoCl_2$	*Sirt1*+/+ (n=5)	5	0	0	0	0
	Sirt1-/- (n=6)	0	4 (1 out of 4 with ASD)	1 (with ASD)	1	0
	Sirt1 WT (n=6) (*Sirt1*$^{fl/+}$*Isl1-Cre*^{neg})	6	0	0	0	0
	Sirt1 conditional null mutants (n=7) (Sirt1$^{fl/fl}$Isl1-Cre^{pos})	5	2	0	0	0
+$CoCl_2$	*Sirt1* WT (n=8) (*Sirt1*$^{fl/+}$*Isl1-Cre*^{neg})	2	2 (with OA/VSD)	2	4	2 (with OA/VSD)
	Sirt1 heterozygotes mutants (n=11)	11	0	0	0	0
	Sirt1 conditional null mutants (n=8)	8	0	0	0	0

Suppl. Table 2: Incidence of cardiac structural defects in embryos lacking Sirt1 in the SHF with and without $CoCl_2$ treatment. Summary of cardiac structural defects in wildtype (Sirt1$^{+/+}$; Sirt1$^{fl/+}$/Isl1-Cre^{neg}), heterozygous (Sirt1$^{fl/-}$/Isl1-Cre^{neg}; Sirt1$^{fl/+}$/Isl1-Cre^{pos}) and homozygous (Sirt1$^{-/-}$; Sirt1$^{fl/-}$/Isl1-Cre^{pos}) Sirt1 mutant embryos detected by H&E staining of paraffin sections from E15.5 mouse hearts without (11 embryos from 3 litters mated for germline null embryos and 13 embryos from 4 litters mated for conditional null embryos) or with (27 embryos from 4 litters) $CoCl_2$ treatment. The incidence of different cardiac defects in $CoCl_2$ or untreated hearts with CHDs is indicated. RV: right ventricle; VSD: ventricular septal defect; ASD: atrial septal defect; OA: overriding aorta.

Suppl. Table 3: List of primers used for genotyping, chromatinIP and mutagenesis in the study

Name	Primer sequence (5'-->3')	Application
mSirt1loxP P3 F	GGCAGTATGTGGCAGATT	Floxed and deleted Sirt1 genotyping
mSirt1loxP P4 R	CCTGAAACAGACAAGACCT	Floxed Sirt1 genotyping
mSirt1loxP P6 R	GAACATAACAGCCAGGCAT	Deleted Sirt1 genotyping
Isl1F	ACTATTTGCCACCTAGCCACAGCA	Isl1-Cre genotyping
Isl1R	AATTCACACCAAACATGCAAGCTG	Isl1-Cre genotyping
CreR	CTAGAGCCTGTTTTGCACGTTC	Isl1-Cre genotyping
Nkx2.5F	TAAACTGGTCGAGCGATGGATTTCC	Nkx2.5-Cre genotyping
Nkx2.5R	CATATCTCGCGCGGCTCCGACACGG	Nkx2.5-Cre genotyping
nGFPF	CTCTTGATTCCCACTTTGTGGTTC	Isl1-nGFP genotyping
nGFPR	TCAGTAAGCTATGGGTTAGAG	Isl1-nGFP genotyping
Isl1ISHF	GGTCCCGAGCCGTGCAGGTCC	DNA probe for ISH
Isl1ISHR	GCGCGCTGGATGCAAGGGACTG	DNA probe for ISH
Hes1mF	GGACCTACCGTCGACCTACTCGCCACGGGCGGCAG	Mutagenesis
Hes1mR	GGCGAGTAGGTCGACGGTAGGTCCTTCCTGTG	Mutagenesis
Isl1P-KpnI	GGTACCTTGGAGAGCTCAGATTGG	Luciferase reporter
Isl1P-HindIII	AAGCTTATCTGTAAGAGGGAGTAATG	Luciferase reporter
HA-Nkx2.5	CTAGCTAGCACGATGTACCCATACGATGTTCCAGAT TACGCTTTCCCCAGCCCTGCGCTC	Nkx2.5 expression vector
Nkx2.5-V5	ACGCGTCGACCTACGTAGAGTCGAGACCGAGGAGA GGGTTAGGGATAGGCTTACCCCAGGCTCGGATGCCG	Nkx2.5 expression vector
Isl1p-2940	GCGCCAGGAACTGTGCTCCAA AGGGGCGACCTCTTGTGTTCAATG	ChIP
Isl1p-850	GAACAGGAGACCTCACGGGTCGGG CTAGCAGCGCGCTACGCGTTAGGG	ChIP
Nkx2.5p-4604	TTTCTCAACCTTTTCGCCTATTCA GTTTTCTCCACCCCTTCATCTG	ChIP
Nkx2.5p-9556	GTGCCCCAGTGACCCGCTCCAT TATCTCCCTTCCCCGCTGTTGTCC	ChIP
Nkx2.5p-2581	AGGCAAAGAAATCACTCCACA TGTTACAATGGCTGGGAA	ChIP

Suppl. Table 4: List of primers used for qPCR in the study

Name	Primers	Application	Ta (ºC)	Efficiency (%)	Amplicon size (bp)	Position (start)
Isl1	CTGCGGGAGGATGGGCTTTTCT GGTCTTCTCCGGCTGCTTGTGG	qRT	61	97	179	631
Flk1	GGGATGGTCCTTGCATCAGAA ACTGGTAGCCACTGGTCTGGTTG	qRT	58	100	139	4036
Nkx2.5	ACCTTTCTCCGATCCATCCCACT GCGTTAGCGCACTCACTTTAATG	qRT	58	100	227	1504
CD31	GCTCATTGCGGTGGTTGTCAT CATCTCCACGGGTTTCTGTTTG	qRT	58	95	106	2003
Myh11	CGCCCAGAAAAACAATGCCCTAAA GCGTATCCTCCAGCTCCGTCTTGA	qRT	61	100	167	3458
Myh6	GCCCAGTACCTCCGAAAGTC GCCTTAACATACTCCTCCTTGTC	qRT	61	100	110	239
Hand1	AAGACTCTGCGCCTGGCTACCA CGCCCTTTAATCCTCTTCTCGC	qRT	61	98	205	761
Hand2	ACTCAGAGCATCAACAGCGCCTTC TGTGCTTTTCAAGATCTCATTCAGCTC	qRT	61	95	242	1258
Mef2c	GAGCAGTTCTGTGTTCTTTTGC ATCCCTCTGCACAAGTGTCTG	qRT	53	96	129	1
Tbx5	ACTGGCCTTAATCCCAAAAC GGTGAGTTTGAGCTT CTGGA	qRT	53	100	210	927
Sma	TCAGCGCCTCCAGTTCCT AAAAAAAACCACGAGTAACAAATCAA	qRT	56	100	69	1289
Myh7	GCCAACACCAACCTGTCCAAGTTC TGCAAAGGCTCCAGGTCTGAGGGC	qRT	63	100	179	5806
β-actin	CATGAAGATCCTGACCGAGCGTGG TGCTCGAAGTCTAGAGCAACATAGC	qRT	61	95	108	676
Sirt1	GCAGGTTGCAGGAATCCAA GGCAAGATGCTGTTGCAAA	qRT	55	98	62	1094
36b4	TCCAGGCTTTGGGCATCA CTTTATCAGCTGCACATCACTCAGA	qRT	56	100	74	534
Isl1p-468	AAAGCGGCCCGTTCCAAGTGC GCGCCGCGTCGTGTCCTG	ChIP	61*	99	178	-468
Nkx2.5p-9040	AAAGTCCCCGCGAGTGTTGTGT TTGGTGAAAAGCGGGATGGAGACG	ChIP	61*	100	183	- 9040
Nkx2.5p-4604	TTTCTCAACCTTTTCGCCTATTCA GTTTTCTCCACCCCTTCATCTG	ChIP	61	93	234	- 4604
Nkx2.5p-9556	GTGCCCCAGTGACCCGCTCCAT TATCTCCCTTCCCCGCTGTTGTCC	ChIP	63	100	201	- 9556
Nkx2.5p-2581	AGGCAAAGAAATCACTCCACA TGTTACAATGGCTGGGAA	ChIP	55	93	155	- 2581

qRT: Real-Time Quantitative Reverse Transcription PCR; *: PCR contains 4% DMSO.

Suppl. Table 5: List of antibodies used in the study.

Antibody	Use	Use Supplier	Cat. No.
Histone H3	WB, ChIP	Abcam	ab1791
H3K9ac	WB, ChIP	Abcam	ab4441
H4K16ac	ChIP	Abcam	ab10158
Isl1	IF, WB, ChIP	Hybridoma Bank	39.4D5
Nkx2.5	IF, WB	Abcam	ab35842
Nkx2.5	WB	Santa Cruz	Sc-376565
V5	WB	Abcam	Ab9116
HIF1α	WB, IP	Bethyl	A300-286A
HIF1α	ChIP	Novus Biologicals	NB100-134
CD31-APC	FACS	eBioscience	17-0311
cTNT	FACS	Abcam	ab8295
Myh11-PE	FACS	Santa Cruz Biotechnology	sc-6956
Flk1-PE	FACS	BD Biosciences	555308
Sirt1	IF, WB, IP	Cell signaling	2028
Sirt1	ChIP	Millipore	07-131
pHistone 3	IF	Cell signaling	9701
Hes1	WB, IP	Santa Cruz	sc-25392
JNK 1/2	WB	Cell signaling	9258
pJNK1/2	WB	Cell signaling	9251
α-Tubulin	WB	Sigma	T6074
α-sarc.-Actinin	WB	Sigma	A7811
α-Actin	WB	Sigma	A5441
M2(Flag)	WB, IP	Sigma	A2220
Myc	WB, IP	Cell signaling	2278
HDAC1	WB, ChIP	Cell signaling	5356
HDAC5	WB, ChIP	Active Motif	40970

IF: Immunofluorescence, WB: Western blot, IP: immunoprecipitation, ChIP: Chromatin